

## Microstructure evolution of Ferritic ODS steel by a simple torsion test

Hyun Ju Jin\*, Suk Hoon Kang, Sang Min Park and Tae Kyu Kim

Nuclear Materials Division, Korea Atomic Energy Research Institute, Yuseong-gu, Daejeon, Republic of Korea

\*Corresponding author: hjin@kaeri.re.kr

### 1. Introduction

Oxide dispersion strengthened (ODS) ferritic steels are considered a promising candidate material for high-temperature components operating in aggressive environments such as nuclear fusion and fission systems owing to their excellent high-temperature strength, corrosion and radiation resistance [1-3]. These characteristics originate from microstructures consisting of fine grains and nano-oxide particles dispersed in high a number density. In particular, the grain size is a key structural factor affecting nearly all aspects of the physical, chemical, and mechanical behavior of metals. While many studies have been made on microstructure evolution for austenitic ODS steels, the microstructure evolution of ferritic ODS steels related to the deformation mechanism has not yet been clearly understood.

This study investigates the microstructural evolution and microhardness of ferritic ODS steel during forward and reverse shear strain by using a torsion test. The microstructures were observed using electron back-scatter diffraction (EBSD) and transmission electron microscopy (TEM).

### 2. Methods and Results

#### 2.1 Methods

The work presented here focused on ferritic ODS steel, the chemical composition of which is given in Table I.

Table I. Chemical composition (wt. %) of 15Cr ODS steel.

Cr	Mo	Ti	Y <sub>2</sub> O <sub>3</sub>	Fe
15	1	0.3	0.35	Bal.

It has been widely known that ODS steels are made through a mechanical alloying (MA) process [4,5]. Accordingly, MA was carried out with elemental metal powders along with 0.35 wt% Y<sub>2</sub>O<sub>3</sub> powders in a high energy miller (CM 20) at a rotation speed of 240 rpm for 48 hours at room temperature. The MA powders were placed in an AISI 304L stainless steel container, sealed after a degassing process, and consolidated by a hot isostatic pressing process at 1150°C under a pressure of 100 MPa for 3 hours. The hiped bars were hot-rolled at 1150°C into a plate with a reduction ratio of 40%.

Fig.1 (a) shows a schematic design of the specimen used for the simple torsion test. The total shear strain,  $\gamma$ , was acquired by a change in the black line marked on the gage section of the specimen after torsion and/or torsion-reverse torsion, as shown in Fig.1.(b) and (c). In the case of forward torsion, the total shear strains that we controlled were 0, 0.16, 0.33, 0.65, and 1.0. For torsion-reverse torsion, the specimens were shear-strained by 0.16, 0.33, and 1.0, and then reverse-torsioned at the same amount of shear strain as depicted in Fig.1 (c).

The microstructure evolution was observed through EBSD (Oxford INCA). The EBSD specimens were prepared using electro polishing in the gage section, which is a surface perpendicular to the radius. Microstructural characterization of the dislocations and oxide particles was carried out using a high resolution TEM (JEM 2100F). The thin foil specimens for TEM observation were prepared through jet-polishing using 5% HClO<sub>4</sub> + 95% CH<sub>3</sub>OH at 25V at -40°C. Microhardness profiles were measured on the surface perpendicular to the radius using a Vickers microhardness tester with a 0.5kgf load for 15 s.

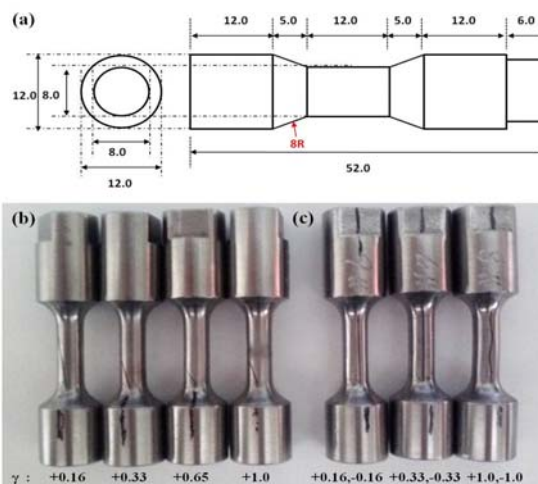


Fig.1. Schematic illustration and images of the specimen for a simple torsion test. (a) layout of the specimen for torsion test, and images illustrating the (b) torsioned and (c) torsion-reverse-torsioned ferritic ODS steels.

#### 2.2 Results

Fig.2 shows the Vickers hardness profiles of ferritic ODS samples with shear strain amounts for only forward torsion and with shear strain mode. It was found that the hardness value increased during shear

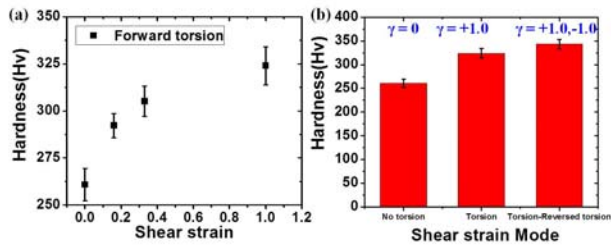


Fig.2. Microhardness values of ferritic ODS steel samples (a) with shear strain amounts for only forward simple shear deformation (forward torsion) and (b) with shear strain mode.

deformation, indicating that the increase in hardness is associated with the strain hardening mechanism by the deformation. Notice that, as depicted in Fig.2 (b), there was an additional increase in hardness when the sample was reverse-torsioned after a forward torsion, suggesting that the hardening of ferritic ODS steel is influenced by the shear strain path as well as the shear strain amounts.

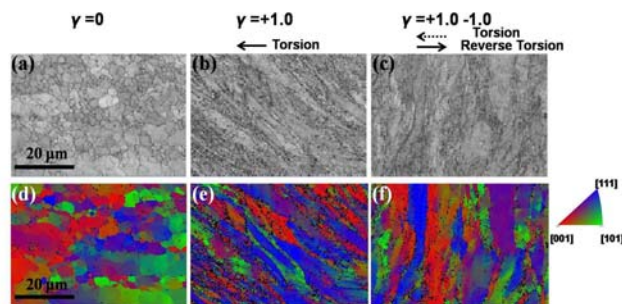


Fig.3. EBSD images of microstructure evolutions during simple shearing, (a) as hot-rolled (b) torsioned ( $\gamma=+1.0$ ) and (c) torsion-reverse torsioned ( $\gamma=+1.0, -1.0$ ) ferritic ODS steel.

Fig. 3 exhibits the microstructure evolutions during the simple shearing of ferritic ODS steel. The deformed microstructures were observed by EBSD band contrast maps and orientation maps in the perpendicular plane to the radius. The microstructure of ferritic ODS steel after the hot-rolling process is presented in Figs.3 (a) and 3 (d) as a reference, showing inhomogeneous grain distributions. In Fig.3 (b), when ferritic ODS steel was subjected to forward shear strain, the shear deformed microstructures were observed, and refined grains of several hundred nanometers in size were identified including elongated grains along the shear band direction. It was also found that a high fraction of red and blue regions representing  $\langle 100 \rangle$  and  $\langle 111 \rangle$  textures were developed, respectively, as shown in Fig.3 (e). Such distributions are related to the evolution of typical BCC rolling/torsion textures [6]. Figs.3(c) and 3(f) present the microstructure of ferritic ODS steel experienced in reverse torsion after forward torsion. While the grains were refined to hundreds of nanometers in size, few specifically preferred orientations were observed. Furthermore, the fraction of  $\langle 111 \rangle$  textures was partially reduced. Accordingly, considering that the hardness value was higher in torsion, and then reverse torsion, as depicted in Fig. 2(b), even through an alteration in the shear strain path,

a continuous generation of cell structures of dislocation entanglement is expected, resulting in a rise in hardness.

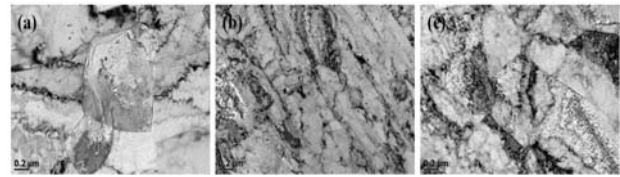


Fig.4. TEM images of (a) as hot-rolled, (b) torsioned ( $\gamma=+1.0$ ), and (c) torsion-reverse torsioned ( $\gamma=+1.0, -1.0$ ) ferritic ODS steel

To understand the influence of both oxide particles and dislocations during shear deformation, TEM observations were performed before and after the torsion test. The bright field TEM images of (a) hot-rolled, (b) torsioned ( $\gamma=+1.0$ ), and (c) torsion-reverse torsioned ( $\gamma=+1.0, -1.0$ ) ferritic ODS steel are shown in Fig. 4. In both torsioned and torsion-reverse torsioned ferritic ODS steels as shown in Fig.4 (b) and (c), a number of cell structures with a dislocation entanglement were identified, leading to an increase in hardness. The subdivided grains can be attributed to fine oxide particles during shearing.

### 3. Conclusions

The microstructural evolution and microhardness of ferritic ODS steel during forward and reverse shear strain were investigated. Grain refinement with shear strain resulted in an increase in hardness. The change in shear strain path reduced the anisotropy, yet made the hardness value to higher owing to the formation of cell structures of dislocation entanglement inside the grain.

### ACKNOWLEDGEMENT

This work was supported by the National Research Foundation of Korea (NRF) grant funded by the Korea government(2012M2A8A1027872)

### REFERENCES

- [1] R.L. Klueh, P.J. Maziasz, I.S. Kim, L. Heatherly, D.T. Hoelzer, N. Hashimoto, E.A. Kenik, K. Miyahara, J. Nucl. Mater. 307 (2002) 773–777.
- [2] A. Alamo, V. Lambard, X. Averty, M.H. Mathon, J. Nucl. Mater. 329 (2004) 333–337.
- [3] J. Malaplate, F. Momprou, J.L. Béchade, T. Van Den Berghe, M. Ratti, J. Nucl. Mater. 405 (2011) 95–100.
- [4] R. Schäublin, A. Ramar, N. Baluc, V. de Castro, M.A. Monge, J. Nucl. Mater. 351 (2006) 247–260.
- [5] M.B. Toloczko, D.S. Gelles, F.A. Garner, R.J. Kurtz, K. Abe, J. Nucl. Mater. 329–333 (2004) 352–355. [5] M.B. Toloczko, D.S. Gelles, F.A. Garner, R.J. Kurtz, K. Abe, J. Nucl. Mater. 329–333 (2004) 352–355.
- [6] U.F. Kocks, C.N. Tome and H.-R. Wenk, Texture and Anisotropy, 1998, p.201; Cambridge University Press.